7

Interference Effects of Excess Ca, Ba and Sr on Mg Absorbance During Flame Atomic Absorption Spectrometry: Characterization in Terms of a Simplified Collisional Rate Model

Mark F. Zaranyika[1], Albert T. Chirenje[1]
and Courtie Mahamadi[2]
[1]*Chemistry Department, University of Zimbabwe, Mt Pleasant, Harare,*
[2]*Chemistry Department, Bindura University of Science Education, Bindura,*
Zimbabwe

1. Introduction

Group II elements constitute an environmentally important group of metals. Calcium ranks 5th in relative abundance in nature. It occurs in limestone, dolomite, gypsum and gypsiferous shale, from which it can leach into underground and surface waters. Calcium content of natural waters can range from zero to several hundred milligrams per liter, depending on the source and treatment of the water. Magnesium occurs in nature in close association with calcium. It ranks 8th in abundance among the elements, and is a common constituent of natural waters. As with calcium, concentrations of magnesium in natural water may vary from zero to several hundred milligrams per litre, depending on source and treatment of the water. Calcium and magnesium salts contribute to water hardness. Concentrations of Mg above 125 mg/L can have cathartic and diuretic effects on the water (APHA, 1992). Barium ranks 16th in relative abundance in nature, and occurs in trace amounts in natural waters. Strontium resembles calcium, and interferes in the determination of calcium by gravimetric and titrimetric methods. Although most portable water supplies contain little strontium, levels as high as 39 mg/L have been detected in well water (APHA, 1992).

FAAS and ICP-AES are the preferred methods for determining Gp II elements including Mg. Signal enhancement and/or depression were reported previous when Gp II elements were determined by atomic absorption spectrometry in the presence of other Gp II elements as interferents by several authors (Zadgorska and Krasnobaeva, 1977; Czobik and Matousek, 1978; Kos'cielniak and Parczewski, 1982; Smith and Browner, 1984; Zaranyika and Chirenje, 1999). Our approach to the study of interelement effects in atomic spectrometry involves a technique of probing changes in the number densities of the excited and ground states. Experimental analyte line emission intensity (I) and line absorbance (A) signal ratios, I′/I and A′/A, respectively, where the prime denotes readings taken in the presence of the interferent, are determined and compared to theoretical values derived assuming steady state kinetics. The method was used to follow collisional processes on the excitation and

ionization of K resulting from the presence excess Na as interferent (Zaranyika et al., 1991). The approach assumes no change in the rate of introduction of analyte atoms into the excitation source, and no change in the temperature of the torch or flame, upon the simultaneous introduction of an easily ionized interferent element.

Our argument is that according to the local thermodynamic equilibrium (LTE) approach, atomic line absorption and atomic line emission intensities are directly proportional to the population of the ground and excited states, respectively, i.e., $A \propto N_0$ and $I \propto N_j$ whereas N_j and N_0 are related by the Boltzmann equation (Boumans, 1966):

$$N_j = N_o . \left(\frac{g_j}{g_o} \right) \exp\left(-\Delta E / kT \right) \tag{1}$$

where g_j and g_0 are the statistical weights of the excited and ground states, respectively, k is the Boltzmann constant, T is the absolute temperature and ΔE is the difference in the energies of the two electronic states involved in the transition. If the rate of introduction of the analyte atoms into the plasma is kept constant, and we assume no change in the plasma temperature on simultaneous introduction of interfering metal atoms with the analyte, we may write:

$$N_j' = N_o' \left(\frac{g_j}{g_o} \right) \exp\left(-\Delta E / kT \right) \tag{2}$$

where the primes denote the actual populations of analyte ground state and excited atoms in the presence of the interferent. Combining equations 1 and 2, we have

$$\frac{N_j'}{N_j} = \frac{N_o'}{N_o} \tag{3}$$

Hence,

$$\frac{I'}{I} = \frac{A'}{A} = \frac{n_u'}{n_u} \tag{4}$$

where n_u is number density of the excited state.

Equation 4 suggests that the effects of collisional processes on the excitation, and line emission of the analyte atoms resulting from the presence of interferent atoms may be followed by measuring the absorption or emission intensities of a given concentration of analyte atoms in the absence and presence of the interferent, and comparing the I′/I and A′/A ratios plotted versus analyte concentration. Applying the approach to absorption spectrometry, the following situations may be identified:

i. No collisional effects, and therefore no change in the populations of the ground and excited states of analyte atoms: A′/A=1
ii. Increase of ground state, e.g. suppression of ionization: A′/A>1
iii. Depopulation of ground state, e.g. charge transfer reactions: A′/A<1
iv. Increase in excited state population: A′/A>1
v. Depopulation of excited state: A′/A<1

The aims of the present work were to investigate and characterize, in terms of a simplified collisional rate model, the interference effects observed when Mg is determined by air-acetylene FAAS in the presence of excess Ca and Sr as interferents.

2. Experimental

2.1 Equipment

An AA-6401 Shimadzu Spectrophotometer with an aberration-corrected Czerney-Turner mounted monochromator, automatic two step gain adjustment beam balance, automatic baseline drift correction using electrical double beam signal processing in peak height and area modes, was used in conjunction with an air-cooled 100-mm slot burner with a stainless steel head with a Pt-Ir capillary nebulizer with a Teflon orifice, glass impact bead and polypropylene chamber, and an air-acetylene flame. The air was supplied by a Toshiba Toscon compressor at 0.35 MPa input pressure, while the fuel gas was supplied from a pressuresed tank (BOC Zimbabwe (Pvt) Ltd, Harare), at 2.0 mL/min. Under these conditions the temperature of the flame was approximately 2573K [3-5], confirmed by a personal communication obtained from Shimadzu Inc., Japan. The spectrophotometer is equipped with automatic fuel gas flow rate optimization for each element.

Experiments were carried out using Hamamatsu Photonics hollow cathode lamps (Hamamatsu, Japan) as source. The lamps was operated at the recommended minimum current of 8 mA for Mg respectively. Measurements were made using the 285.2 nm Mg line. The spectrophotometer employs a high speed 2-wavelength simultaneous measurement Deuterium lamp to correct for background signal.

The nebulization chamber of the spectrophotometer was cleaned with triply distilled water to remove any deposited solids after each set of runs. The instrument was optimized for absorbance measurements, and care was taken not to change the instrumental settings/conditions until all measurements involving a particular interferent were completed. The average absorbance reading was recorded on the instrument computer monitor 5 seconds after aspiration.

Instrumental parameters employed were as follows: Spectral band pass, 0.5 nm; Burner height, 7 mm; Burner angle, 0^{o}; Acetylene fuel flow rate, 2.0 L/min.; Air input pressure, 0.35 MPa. Minimum Hollow cathode lamp current 8 mA. A mean aspiration rate of 3.00±0.06 mL/min. (n = 8), and mean nebulization efficiency of 6.3±1.7%
(n = 8) were obtained.

2.2 Materials

The following were used: Calcium chloride AR grade (impurities present: sulphate 0.005%, total nitrogen 0.005%, phosphorous 0.001%, lead 0.001%, iron 0.0005%, magnesium 0.01%, sodium 0.01% and potassium 0.01%); magnesium chloride AR grade (impurities: free acid 0.001%, magnesium oxide 0.0005%, nitrogen compounds 0.0002%, arsenic 0.0001%, barium 0.0002%, calcium 0.00055%, potassium 0.005%, sodium 0.0055%, and zinc 0.0025%); Strontium chloride AR grade (impurities: water insoluble matter 0.005%, sulphate 0.001%, lead 0.0002%, iron 0.0001%, zinc 0.0001%, barium 0.02%, and substances not precipitated by sulphuric acid 0.0002%); Deionized water of conductivity 0.001μSm-1.

2.3 Procedure

Four sets of standard solutions each containing 1 – 30 mg/L Mg were prepared from a freshly prepared stock solution. Three sets were spiked with 1000 mg/L Ca or Sr each

respectively; while one set each was left unspiked. The concentration of the interferent was kept in excess at 1000 mg/L while that of the analyte was kept at 0 -30 mg/L to minimize changes in the physical properties of the test solution. Any such changes in physical properties would affect the set of solutions to be analyzed to the same extent, and this was compensated for by taking blank readings of the solution containing the interferent only.
Absorbance (A) readings were made for the spiked sets of solutions, as well as the unspiked set using distilled water as blank. The readings for the spiked sets of Mg solutions were then adjusted for blank readings of the solution containing the interferent only. A'/A ratios were calculated and plotted against Mg concentration in the test solution in Figure 1. Preliminary experiments were run to determine the aspiration rate and nebulization efficiency for the type of solutions under analysis. A mean aspiration rate (n = 8) of 3.00±0.06 mL/min and a mean nebulization efficiency (n = 8) of 6.3±1.7% were obtained.

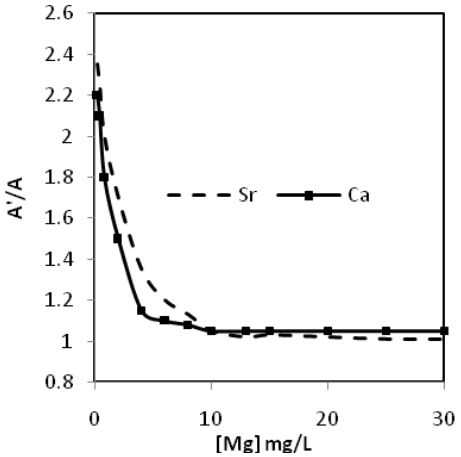

Fig. 1. Interference effects of excess Ca and Sr on Mg absorbance during air-acetylene FAAS.

2.4 Theoretical calculations

Ground state number densities were calculated assuming an aspiration rate of 3 mL/min. and 6 % nebulization efficiency as measured above, and a temperature of 2573 K for the air-acetylene flame as noted above. Ionic number densities were calculated on the basis of the Saha relationship (Allen, 1955). Data obtained are shown in Table 1, in column headed 'n_o ($cm^{-3}s^{-1}$)'.

M	n_o ($cm^{-3}s^{-1}$)	n_+(or n_{m+}) ($cm^{-3}s^{-1}$)[a]	[a]	n_{e^*} ($cm^{-3}s^{-1}$)
Mg	$2.5154 \times 10^{12}c$	$1.8252 \times 10^{9}c^{1/2}$		$1.8252 \times 10^{9}c^{1/2}$
Ca	2.5431×10^{14}	5.6225×10^{11}	0.002	5.5859×10^{8}
Sr	8.3084×10^{14}	2.5694×10^{12}	0.003	3.8571×10^{8}

[a]Based on Saha relationship. M = element; α = degree of ionization assuming 2573 K flame temperature. c = analyte concentration in the test solution.

Table 1. Ground state atom, ion and pre-thermal equilibration "hot" electron number densities, n_{e^*}.

3. Results and discussion

The experimental A′/A curves in Fig. 1 show a sharp increase in line absorbance signal enhancement with decrease in the concentration of the analyte in the test solution below about 10 mg/L. Similar results were reported previously in a study of mutual atomization interference effects between Group I elements (Zaranyika and Makuhunga, 1997). Absorbance signal enhancement is attributed to suppression of ionization, which is equivalent to collisional ion-electron radiative recombination. The major processes affecting analyte ground state population in the flame are represented schematically in Fig. 2.

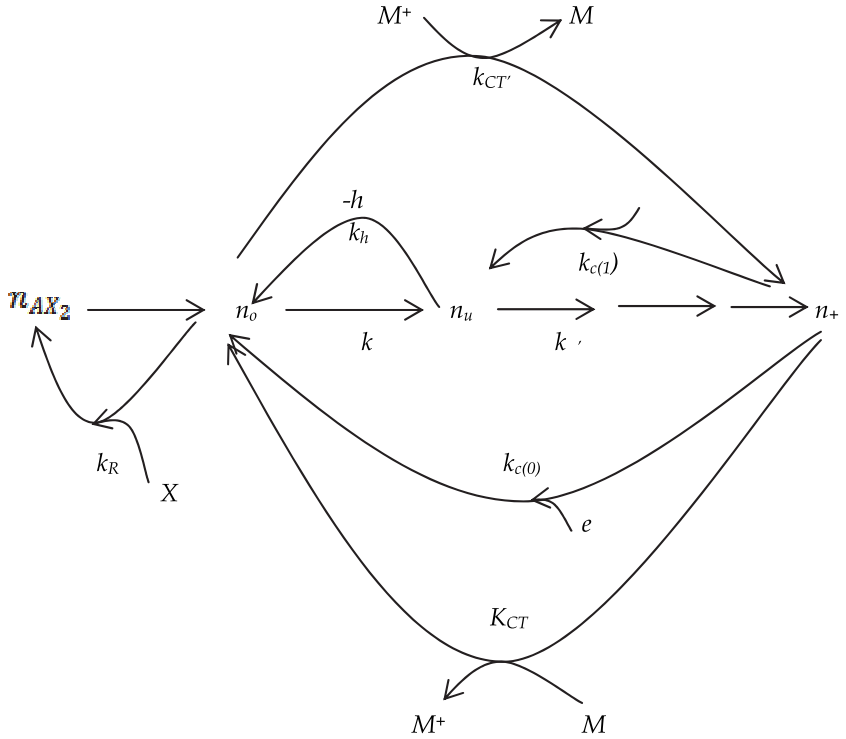

Fig. 2. Proposed kinetic scheme: The subscripts AX2, o, u, and + denote analyte salt, ground state, excited state and ion respectively; M denotes interferent; k_D, k_Δ, k_Δ' denote rate constants for thermal dissociation, excitation from the ground state and excitation the excited state respectively; k_{CT} and $k_{CT'}$ denote rate constants for collisional charge transfer involving interferent atoms and ions respectively; $k_{c(o)}$ and $k_{c(1)}$ denote rate constants for collisional radiative recombination to the ground state and excited state respectively; $k_{h\nu}$ and k_R denote rate constants for radiative relaxation and analyte atom and counter- atom recombination respectively.

Assuming a steady state with respect to the analyte ground state and the excited state:

$$\frac{dn_A}{dt} = k_D n_{AX_2} + k_{c(o)} n_u n'_e + k_{CT} n_+ n_{Mo} + k_{h\nu} n'_u - k_\varphi n'_o - k'_{CT} n_o n_{M+} - k_R n'_o n_X = 0 \qquad (5)$$

$$\frac{dn_u}{dt} = k_\phi n'_o - k_{hv} n'_u - k'_\Delta n'_u = 0 \tag{6}$$

Rearranging Eq. 6, we have

$$k_{hv} n'_u = \left(\frac{k_{hv}}{k_{hv} + k'_\Delta} \right) k_\phi n'_o \tag{7}$$

Substituting into Eq. 5 and rearranging:

$$n'_o = \frac{k_D n_{AX_2} + k_{CR(o)} n_+ n'_e + k_{CT} n_+ n_{mo}}{k'_{CT} n_{m+} + k_R n'_X + k_\phi \left(1 - \frac{k_{hv}}{k_{hv} + k'_\Delta} \right)} \tag{8}$$

$$n'_o = \frac{k_D n_{AX_2} + k_{CR(o)} n_+ n'_e + k_{CT} n_+ n_{mo}}{k'_{CT} n_{m+} + k_R n'_X + k'_\phi} \tag{9}$$

Where

$$k'_\phi = k_\phi \left(1 - \frac{k_{hv}}{k_{hv} + k'_\Delta} \right) \tag{10}$$

Therefore

$$\frac{n'_o}{n_o} = \left[\frac{k_D n_{AX_2} + k_{CR(o)} n_+ n'_e + k_{CT} n_+ n_{mo}}{k_D n_{AX_2} + k_{CR(o)} n_+ n_e} \right] \left(\frac{k'_\phi + k_R n_X}{k'_\phi + k'_{CT} n_{m+} + k_R n'_X} \right) \tag{11}$$

Two major limiting cases can be defined for Eq. 11, thus:
Limiting Case I (LC I):

$$k_D n_{AX2} \succ\succ k_{CR(o)} n_+ n'_e + k_{CT} n_+ n_{mo}$$

$$\frac{n'_o}{n_o} = \frac{k'_\phi + k_R n_X}{k'_\phi + k'_{CT} n_{m+} + k_R n'_X} \tag{12}$$

Since $k_R n_X' >> k_R n_X$, n_o'/n_o will be less than unity, i. e., a depression of absorbency signal is expected in this case, contrary to the experimental results in Fig. 1. Although the present work reports analyte line absorption signal enhancement, analyte line absorption signal depression has been reported by several workers (Herrmann and Alkemade, 1963; Brown et al., 1987). Analyte line absorption signal depression conforming to Eq. 12 was also reported previously at low flame temperature when 0.2 – 1.0 mg/L K solutions were determined in the presence of 1000 mg/L Na in the secondary reaction zones of the air-acetylene flame (Zaranyika et al., 1991).

Limiting Case II (LC II):

$$k_D n_{AX2} \prec\prec k_{CR(o)} n_+ n_e$$

$$\frac{n_o'}{n_o} = \left[\frac{k_{CR(o)}n_+n_e' + k_{CT}n_+n_{mo}}{k_{CR(o)}n_+n_e}\right]\left(\frac{k_\phi' + k_R n_X}{k_\phi' + k_{CT}'n_{m+} + k_R n_X'}\right) \tag{13}$$

Two further limiting cases can be defined for Eq. 13, thus:
Limiting Case IIA (LC IIA):

$$k_\varphi' \succ\succ k_{CT}'n_{m+} + k_R n_X'$$

$$\frac{n_o'}{n_o} = \frac{k_{CR(o)}n_+n_e' + k_{CT}n_+n_{mo}}{k_{CR(o)}n_+n_e} \tag{14}$$

Since $n_e' = n_+ \Delta n_e = n_+ + \alpha n_{mo}$, where Δn_e represents the change in the electron number density in the presence of the interferent, and α is the degree of ionization of the interferent, Eq. 14 becomes

$$\frac{n_o'}{n_o} = 1 + \left(\frac{\alpha k_{CR(o)} + k_{CT}}{k_{CR(o)}}\right)\frac{n_{mo}}{n_+} \tag{15}$$

Or

$$\frac{n_o'}{n_o} = 1 + \frac{kn_{mo}}{n_+} \tag{16}$$

i.e., absorbance signal enhancement is directly proportional to interferent number density and inversely proportional to analyte number density. In addition, if we assume that $A'/A = n_{o'}/n_o$, a plot of A'/A versus n_{mo}/n_+, should be linear with an intercept of unity. At constant interferent concentration in the test solution, a plot of A'/A versus $1/n_+$, should also be linear with an intercept of unity.
Limiting Case IIB (LC IIB):

$$k_\phi' \prec\prec k_R n_X$$

It can be shown that

$$\frac{n_o'}{n_o} = \left\{1 + \left(\frac{\alpha k_{CR(o)} + k_{CT}}{k_{CR(o)}}\right)\frac{n_{mo}}{n_+}\right\}\left(\frac{k_R n_X}{\alpha k_{CT}'n_{mo} + k_R n_X'}\right) \tag{17}$$

i.e., although the absorbance signal enhancement is still dependent on interferent number density and inversely proportional to analyte number density, the enhancement observed will be reduced by a factor of at least n_X/n_X'. In addition, if we assume the $A'/A = n_o'/n_o$, a plot of A'/A versus n_{mo}/n_+ should give a non-linear slope dependent on the concentration of interferent metal atom and counter atom, and with an intercept that is less than unity and equal to at least n_X/n_X'.
Table 2 shows the slope, intercept and R^2 values for the regression plots of A'/A versus n_{mo}/n_+ obtained when the enhancement factor A'/A for Mg is determined in the presence and absence of Ca and Sr as interferents. It is apparent from the data in Table 2 that the

intercept values of 1.09 and 1.22 obtained are close to unity, in close agreement with Eq. 11. These data suggest that the signal enhancement obtained when Mg is determined in the presence of excess of Ca and Sr as interferents conforms to LC IIA.

Interferent	Slope	Intercept	R^2
Ca	2.34×10^{-4}	1.08714	0.909
Sr	3.38×10^{-3}	1.21649	0.732

Table 2. Regression data: A′/A vs n_{mo}/n_+ for Mg

Signal enhancement in the presence of easily ionizable elements (EIEs) in atomic absorption spectrometry is commonly attributed to suppression of ionization (Foster Jr. and Hume, 1959; Smit et al., 1951). Supression of ionization is in effect collisional radiative recombination, and assumes that in Eq. 14 $k_{CR(o)}n_+n_e' \succ\succ k_{CT}n_+n_{mo}$ so that Eq. 14 reduces to

$$\frac{n_o'}{n_o} = \frac{k_{CR(o)}n_+n_e'}{k_{CR(o)}n_+n_e} = 1 + \frac{k_{CR(o)}n_+\Delta n_e}{k_{CR(o)}n_+n_e} \tag{18}$$

Or

$$\frac{n_o'}{n_o} = 1 + \frac{k_c n_+ \Delta n_e \exp(-E_a'/kT)}{k_c n_+ n_e \exp(-E_a/kT)} = 1 + \frac{\Delta n_e \exp(-E_a'/kT)}{n_e \exp(-E_a/kT)} \tag{19}$$

where Δn_e is the change in electron number density upon the addition of the interferent, i.e., $\Delta n_e = n_{m+}$, E_a' and E_a are the activation energies for the electrons from the ionization of the interferent and analyte respectively, and. k_c is the collisional rate constant given by (Weston and Schwarz, 1972):

$$k_c = Q_{12}\left(\frac{8kT}{\pi\mu}\right)^{1/2} \tag{20}$$

where Q_{12} is collision cross-section between particles 1 and 2, and μ is their reduced mass.
If we assume thermal equilibrium conditions, then all the electrons will require the same activation, i.e., $E_a' = E_a$, and Eq. 19 reduces to

$$\frac{n_o'}{n_o} = 1 + \frac{\Delta n_e}{n_e} \tag{21}$$

where $\Delta n_e = n_{m+}$ and $n_e = n_+$. It is apparent that substitution for Δn_e and n_e from Table 1 will yield values of n_o'/n_o up to three orders of magnitude greater than experimental A′/A values at low Mg concentrations. If however we assume pre-thermal equilibrium collisional radiative recombination, then the electrons from the ionization of the interferent would require further activation by an amount of energy equal to the difference between the ionization potentials of the analyte and that of the interferent, i.e., in eq. 19,

$$E_a' = IP_a - IP_m \tag{22}$$

And

$$E_a = IP_a - IP_a = 0 \tag{23}$$

where the subscripts *a* and *m* denote analyte and interferent respectively. If we make this assumption, then Eq. 15 becomes

$$\frac{n_o'}{n_o} = 1 + \frac{\Delta n_e}{n_+}\exp(-E_a' / kT) \tag{24}$$

Table 3 shows the fraction of such electrons having the appropriate energy, and Table 1 shows the corresponding pre-thermal equilibration number density of "hot" electrons, n_e*, arising from the analyte, Mg ($n_e^* = n_+$), and the interferents Ca and Sr ($n_e^* = n_+ \exp(-E_a'/kT)$). *$E_a' = IP_a - IP_m$.

Element	IP_a (eV)	IP_m (eV)	E_a' (eV)*	$\exp(-E_a'/kT)$
Mg	7.644			
Ca		6.111	1.533	9.9349×10^{-4}
Sr		5.692	1.952	1.5012×10^{-4}

Table 3. Pre-thermal equilibration fraction of electrons having the requisite activation energy.

Substitution of the appropriate quantities from Table 1 and 4 into Eq. 24 yields Eqs. 25 and 26 for the absorbance signal enhancement factor, n_o'/n_o, for the presence of 1000 μg/ mL excess Ca and Sr as interferents:

$$\left(\frac{n_o'}{n_o}\right)_{Mg/Ca} = 1 + \frac{3.0604x10^{-1}}{\sqrt{c}} \tag{25}$$

$$\left(\frac{n_o'}{n_o}\right)_{Mg/Sr} = 1 + \frac{2.1132x10^{-1}}{\sqrt{c}} \tag{26}$$

A major objective for kinetic modeling of interference effects is to be able to predict the interference observed experimentally. If assume that

$$\frac{A'}{A} = \frac{n_o'}{n_o} \tag{27}$$

then the calibration curve obtained in the presence of the interferent can be predicted. Theoretical calibration curves predicted on the basis of Eqs 25 and 26 for the effects of 1000 mg/L excess Ca, Br and Sr respectively on the absorbance signal of Mg in the air-acetylene flame are shown in Fig. 3, together with the experimental A′ calibration curves for comparison.

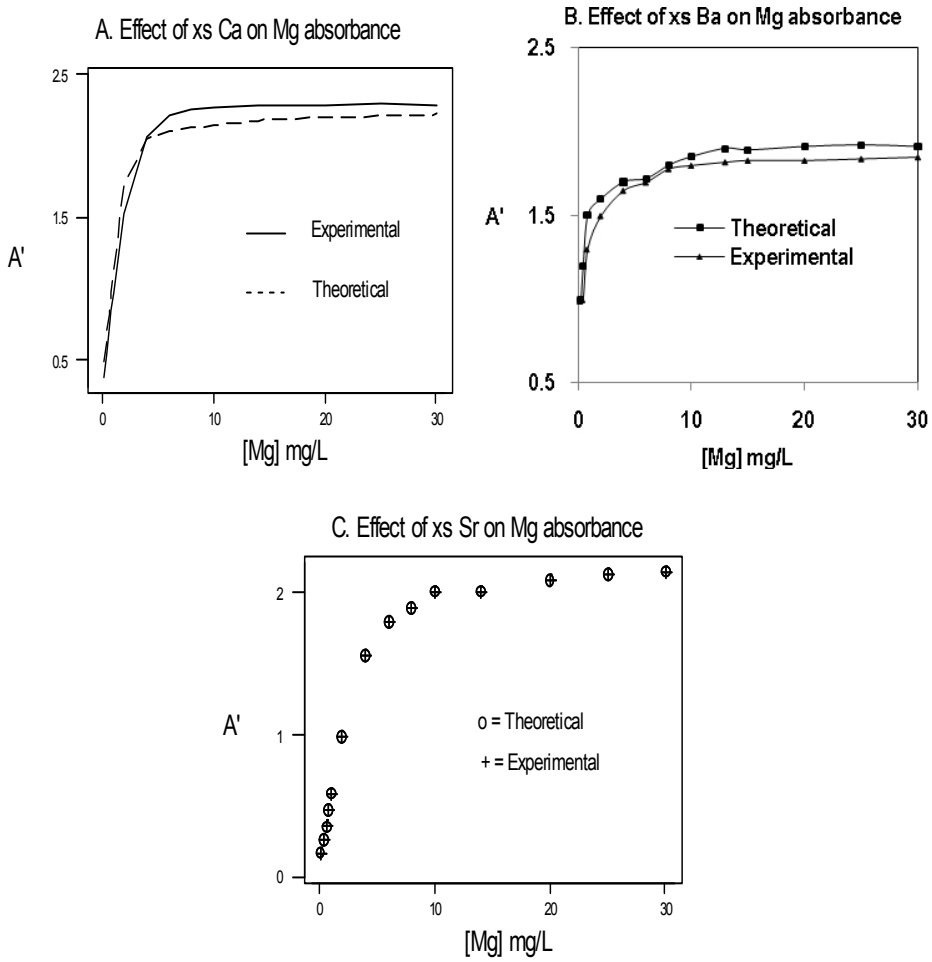

Fig. 3. Theoretical and experimental A′ calibration curves: Effect of excess Ca (A), Ba (B) and Sr (C) on Mg absorbance during air-acetylene FAAS.

It is apparent from Fig. 3A that Eq. 24 leads to close agreement between theory and experiment at Mg concentrations below about 5 mg/L when Mg is determined in the presence of excess Ca, while the theoretical curve deviates slightly from the experimental curve above this concentration. In contrast to the case when Mg is determined in the presence of excess Ca, exact agreement between theory and experiment is obtained throughout the range of Mg concentrations studied when determined in the presence of excess Sr. Although the work presented in this paper is rather limited in scope, the remarkable success of the model in predicting the interference of excess Sr on the absorbance signal of Mg, confirms the potential of the model as represented by Eq. 24 in simulating the absorbance signal enhancement interference effects during flame atomic spectrometry. Further work is underway to test the model on other systems.

4. Conclusions

From the foregoing discussion we conclude that the interference effects between Group II elements can be characterized using a simplified rate model that takes into account collisional radiative recombination, charge transfer between analyte and interferent species, and collisional recombination between analyte atom and counter atom. The model predicts that, depending on the specific experimental conditions employed, interference effects in flame atomic spectrometry can manifest themselves as enhancements (Eq. 15) or depressions (Eqs. 12 and 17) of the analyte line absorbance signal. Data relating to the signal enhancement interference effects of excess Ca and Sr on Mg absorbance signal during air-acetylene flame absorption spectrometry suggest that the signal enhancement can be simulated on the basis of a simplified rate model that assumes pre-LTE ion-electron radiative recombination.

5. Acknowledgements

This work was supported by a grant from the Research Board of the University of Zimbabwe (UZ).

6. References

American Public Health Association (APHA), American Water Works Association (AWWA) and Water Environment Federation (WEF), in Standard Methods for the examination of water and wastewater, 18th Ed., A .E. Greenberg (APHA), L. S. Clesceri (WEF) and A. D. Eaton (AWWA), eds. American Public Health Association, Washington DC, 1992.

Czobik, E.J., and Matousek, J.P., (1978). Interference effects in furnace atomic absorption spectrometry. Analytical Chemistry, 50, 1, 2-10.

Smith, D.D., and Browner, R.F., (1984). Influence of aerosol drop size on signals and interferences in flame atomic absorption spectrometry. Analytical Chemistry, 56, 14, 2702-2708.

Zaranyika, M.F., and Makuhunga, P., (1997). A possible steady state kinetic model for the atomization process during flame atomic spectrometry: Application to mutual atomization interference effects between group I elements. Fresenius Journal of Analytical Chemistry, 357, 249-257.

Allen, C.W., (1955). Astrophysical Quantities, 2nd Ed., Athlone Press, ISBN: 13: 9780387987460, London.

Herrmann, R., and Alkemade, C.T.J., (1963). Chemical analysis by flame photometry. 2nd ed., Interscience Publishers, New York.

Brown, A.A, Roberts, D.J., and Kahokola, K.V., (1987). Methods for improving the sensitivity in flame atomic absorption spectrometry. Journal of Analytical Atomic Spectrometry, 2, 201-204.

Zaranyika, M.F., Nyakonda, C., and Moses, P., (1991). Effect of excess sodium on the excitation of potassium in an air-acetylene flame: a steady state kinetic model which takes into account collisional excitation. Fresenius Journal of Analytical Chemistry, 341, 577-585.

Weston, R.E., Schwarz, H.A., (1972). Chemical Kinetics, Prentice-Hall, ISBN: 9780131286603, New Jersey.

Foster, W.H Jr., and Hume D.N., (1959). Mutual cation interference effects in flame photometry. Analytical Chemistry, 31:2033-2036.

Smit J., Alkamade C.T.J., and Verschure, J.M.C., (1951). A contribution to the development of the flame-photometric determination of sodium and potassium in blood serum. Biochimica ET Biophysica Acta, 6, 508-523.

Zadgorska, Z and Krasnobaeva, N (1977), Influence of the anionic component of the additive on the relative intensity of atomic spectral lines in the analysis of dry residues from solutions, Spectrochim. Acta. 32B, 357-363.

Kos'cielniak, P and Parczewski, A (1982), Theoretical model of alkali metals interferences in flame emission spectrometry, Spectrochim. Acta 37B, 881-887.

Zaranyika, M. F and Chirenje, A. T (1999), A possible steady-state kinetic model for the atomization process during flame atomic spectrometry: Application to atomization interference effects of alumimiun on Group II elements. Fresenius J. Anal. Chem, 364, 208-214.

Boumans, P. W. J. M (1966), Theory of Spectrochemical Excitations, Higler and Watts, London.

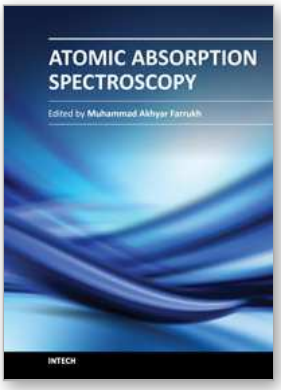

Atomic Absorption Spectroscopy

Edited by Dr. Muhammad Akhyar Farrukh

ISBN 978-953-307-817-5
Hard cover, 258 pages
Publisher InTech
Published online 20, January, 2012
Published in print edition January, 2012

Atomic Absorption Spectroscopy is an analytical technique used for the qualitative and quantitative determination of the elements present in different samples like food, nanomaterials, biomaterials, forensics, and industrial wastes. The main aim of this book is to cover all major topics which are required to equip scholars with the recent advancement in this field. The book is divided into 12 chapters with an emphasis on specific topics. The first two chapters introduce the reader to the subject, it's history, basic principles, instrumentation and sample preparation. Chapter 3 deals with the elemental profiling, functions, biochemistry and potential toxicity of metals, along with comparative techniques. Chapter 4 discusses the importance of sample preparation techniques with the focus on microextraction techniques. Keeping in view the importance of nanomaterials and refractory materials, chapters 5 and 6 highlight the ways to characterize these materials by using AAS. The interference effects between elements are explained in chapter 7. The characterizations of metals in food and biological samples have been given in chapters 8-11. Chapter 12 examines carbon capture and mineral storage with the analysis of metal contents.

InTech Europe
University Campus STeP Ri
Slavka Krautzeka 83/A
51000 Rijeka, Croatia
Phone: +385 (51) 770 447
Fax: +385 (51) 686 166
www.intechopen.com

InTech China
Unit 405, Office Block, Hotel Equatorial Shanghai
No.65, Yan An Road (West), Shanghai, 200040, China
中国上海市延安西路65号上海国际贵都大饭店办公楼405单元
Phone: +86-21-62489820
Fax: +86-21-62489821